

Theory of the relativistic radiative electron capture incorporating effects of the internal conversion process

Ken-ichi Hino* and Tsutomu Watanabe

Atomic Processes Laboratory, The Institute of Physical and Chemical Research (RIKEN), 2-1 Wako-shi, Hirosawa, Saitama 351-01, Japan

(Received 16 May 1988; revised manuscript received 9 November 1988)

We have calculated cross sections of the radiative electron capture into a projectile K -shell orbit (K -REC) by using the relativistic impulse approximation, fully incorporating the internal conversion process, that is, e^+e^- pair creation and successive e^+e^- pair annihilation. The internal conversion process (ICP) is found to play a vital role with an increase of the projectile nuclear charge, while contributions to the ICP from an increase of the relative velocity are less pronounced for, especially, light-ion impacts. Furthermore, the K -REC photon is distributed according to a $\cos^2(\theta_L/2)$ rule with respect to a photon emission angle θ_L in the laboratory frame in the ultrarelativistic energy domain. This feature is quite different from the conventional $\sin^2\theta_L$ dependence, which is valid at most up to an impact velocity below 0.9 of the velocity of light. Calculations are also carried out for the linear polarization correlation of emitted photons using the same approximation. A crossover feature, i.e., a sign inversion of the polarization correlation, comes out in the forward direction relative to 90° with an increase in the impact velocity. This effect is also due to the relativistic effect of the REC.

I. INTRODUCTION

Relativistic effects in radiative electron capture (REC) were first observed in the bombardment of a light projectile ion on a target by Spindler *et al.*¹ Their observation shows that the radiation pattern of K -REC (REC into a K -shell orbit of a projectile ion) has forward-backward symmetry, i.e., the angular distribution of photon emission has a $\sin^2\theta_L$ dependence with respect to an angle θ_L measured from the incident direction in the laboratory frame. This is qualitatively understood as the cancellation of the retardation effect of emitted photons by the aberration effect of the emission angle, i.e., by the Lorentz-transformation effect from the moving frame into the laboratory frame. Anholt *et al.*² also observed a $\sin^2\theta_L$ dependence in the case where a Xe^{54+} ion collides with a Be atom at 197 MeV/ u . Hino and Watanabe³ confirmed theoretically such behaviors of the REC photon angular distributions by employing the relativistic strong-potential Born (SPB) approximation and showed that the radiation pattern of photons is slightly enhanced for the backward direction in the case of 422 MeV/ u U^{92+} colliding on a Be atom because of a strong Coulomb distortion between the ion and the active electron. Furthermore, in contrast to K -REC, L -REC (REC into a projectile L -shell orbit) is asymmetric because the photon retardation corrections do not cancel the aberration effects.⁴

Aside from the photon angular distributions, the relativistic effects of the REC are revealed by observations of the linear polarization correlations of emitted photons as well.⁴ A polarization vector of a photon induced by collisions with nonrelativistic relative velocity always lies on the scattering plane constructed by vectors of the photon

momentum and the incident velocity. This polarization vector gets to turn its direction from on the scattering plane to the plane perpendicular to it with the increase of velocity. Furthermore, the polarization correlation of the photon shows an inversion of its sign at a certain emission angle in the relativistic energy region. This is called a "crossover" feature. According to the Born calculation,⁴ this feature appears in the forward direction relative to 90° when $v/c > 0.8$, with v and c being the relative velocity and the velocity of light, respectively.

Here, we use the words "relativistic effects" associated with the REC process as the combination of the following four issues.

(1) An effect of relativistic incident velocity. This plays an important role to interpret the cancellation effect of K -REC angular distribution and the crossover feature of the polarization correlation in emitted photons mentioned above.

(2) A high-atomic-number (Z_p) effect of highly stripped heavy projectile ions. Here this item has two meanings: one is the relativistic Z_p effect on a K electron captured on a high- Z_p ion and on an intermediate continuum electron, and the other the effect of a strong Coulomb distortion on an active electron. These two Z_p influences cannot be separated in principle in relativistic calculations. The effects are thought to contribute to the backward deviation of the photon angular distribution from the $\sin^2\theta_L$ dependence as indicated on the occasion of the U^{92+} bombardments on Be atoms.

(3) The Lienard-Wichert (LW) potentials⁵ associated with a projectile. The potentials are obtained by taking the Lorentz transformation on a static projectile potential from the moving frame into the rest frame. In this sense, these effects are somewhat related with the relativistic ve-

locity effect of the issue (1). The LW potentials consist of a vector part (space component) and a scalar part (time component), while the original projectile potential has only a scalar part. The vector component of the LW potentials induces spin-orbit couplings of an electron, and the scalar part is intensified by the Lorentz factor $1/[1-(v/c)^2]^{1/2}$ in comparison with the static potential in the projectile frame. Furthermore, the reachable ranges of a projectile potential are widely extended because an electric field ascribable to the LW potential has a component projected onto the direction of the velocity vector as well as that projected onto the direction of the position vector turning from a projectile to an electron. These effects of the LW potentials are expected to become quite pronounced in the relativistic heavy-ion collisions. However, if the reference frame is chosen on a projectile, apparently the LW potentials are replaced by a conventional Coulomb potential. Thus the moving frame is preferred here for simplifying complicated calculations of a REC cross section to some degree, and at the final stage the Lorentz transformation is taken into the rest frame. This transformation introduces all of the effects based on the LW potentials properly and automatically into the final expression of the cross section.

(4) An internal conversion process. Hereafter, this effect is referred to by the acronym ICP. This is herein used to represent the process depicted in the second graph of Fig. 1. The first Feynman diagram shows the conventional REC process. The second diagram indicates the contribution of an intermediate positron. At the first stage, a pair of an electron and a virtual positron is created with an emission of a real photon, successively the positron propagates in the intermediate state, and finally a pair of this positron and an initial electron is annihilated into a virtual photon associated with the Coulomb interaction between an active electron and a

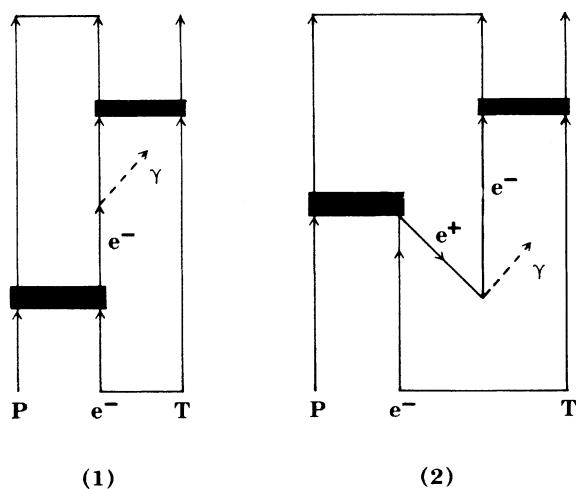


FIG. 1. Feynman diagrams for the relativistic radiative electron capture process. P , T , e^- , and e^+ stand for a projectile ion, a target nucleus, an electron, and a positron, respectively. A bold block represents a Coulomb interaction.

projectile ion. This effect is expected to become very important with the increase of Z_p . This is because the ICP may be interpreted as follows: The strong electric fields due to the existence of a heavy projectile will induce the vacuum polarization cloud around itself. But the time variation of the projectile will partially break up the virtual pairs in collisions into the real e^+e^- pairs.⁶ The electron is converted to a final electron bound on a projectile and, on the other hand, the positron is annihilated with an initial electron. The relativistic effects pointed out in issue (2) should not be separated from the influences of the ICP.

The aims of this article are to investigate the K -REC photon angular distributions, the K -REC total cross sections, and linear polarization correlations of emitted photons up to the ultrarelativistic incident energy region by virtue of the relativistic impulse approximation (RIA) including the whole relativistic effects stated in issues (1)–(4). Above all, we would like to put a stress on the fact that the ICP has not been accounted for in the REC process up to the present time.

Next, we refer to a reason why the impulse approximation (IA) is adopted for the present calculations, not the SPB approximation⁷ which was used in our preceding paper.³ The difference of the SPB from the IA is the presence of the Coulomb off-shell factor. According to Gorriz *et al.*,⁸ the nonrelativistic REC cross section calculated by the SPB approximation is almost double of that by the IA (Ref. 9) because of the presence of this off-shell factor. Following the statements by Jakubassa-Amundsen *et al.*,¹⁰ the photon angular distribution of the REC should be, however, smoothly connected with that of the (two-body) radiative recombination process (RRP) at the on-shell limit, i.e., when the binding energy of a target atom becomes zero. The result of the original SPB approximation does not satisfy this requirement. Jakubassa-Amundsen *et al.* settled this difficulty temporarily by renormalizing the SPB wave function, in other words, by dividing it by a factor ascribable to this discontinuity between the REC and the RRP at the on-shell limit so as to satisfy the requirement of the smooth connection. Further, it is found that the discontinuity of the REC and the RRP is eliminated by incorporating the effect of the asymptotic Coulomb tail with the SPB wave function in accordance with Dollard's idea,¹¹ and the resultant REC cross section then agrees with that by the IA.¹² The same statement is applicable to the cross section of the relativistic REC. Therefore we do not employ the SPB approximation in the present article.

As the end of this section, we will summarize the differences of the preceding formalisms of Refs. 3 and 4 from the present one. First, the RIA formalism is utilized instead of the relativistic SPB approximation because of the statement mentioned to above. Second, the ICP is fully incorporated with the REC transition matrix. The preceding calculation neglected this effect from the beginning of discussion. Third, the ultrarelativistic high-energy limit of the radiation pattern is presented, and, moreover, the linear polarization correlation of an emitted photon is calculated by employing the present method. The latter was evaluated in Ref. 4 by use of the

relativistic plane-wave Born approximation. In addition to these three, we must refer to a theoretical error committed in Ref. 3. In our previous work, the appearance of the Lorentz contraction factor γ^{-2} [Eq. (2.55) of Ref. 3] was emphasized, but this should be replaced by unity. Thus, the results by the relativistic strong-potential Born calculation I (RSPB-I) and the RIA of Ref. 3 must be reduced by γ^{-2} . (However, Figs. 1 and 2 of Ref. 3 are correct because of the normalized values.) For this reason, the RIA result of Ref. 3 differs from the RIA results with no ICP effect (see Figs. 3 and 4) of the present text.

Section II is devoted to formulating the RIA wave function with full consideration of the second Feynman diagram of Fig. 1 as well as the first one. Section III contains calculations of cross sections and linear polarization correlations of emitted photons. Section IV contains results and discussion. The conclusion is in Sec. V. Hereafter, use is made of the natural unit ($\hbar=c=1$) throughout. Moreover, we employ the words "an ultrarelativistic velocity" to denote a velocity which when compared to the velocity of light has a ratio that exceeds 0.9. A kinetic energy of an electron at this ultrarelativistic velocity is larger than its rest mass.

II. WAVE FUNCTION OF THE RIA

We assume the collision system consists of a projectile ion P with an electric charge $Z_P e$, a target nucleus T with

$Z_T e$, and an active electron e with $-e$ for simplicity. The transition matrix of the REC is given by

$$T^{\text{REC}} = -e \langle \Psi_f^{(-)} | \gamma_4 \gamma_\mu A_\mu^* | \Psi_i^{(+)} \rangle \quad (2.1)$$

by using notations of Dirac's γ matrices that $\gamma = -i\beta\alpha$ and $\gamma_4 = \beta$, with α and β being the α and β matrices with respect to an electron. The wave function A_μ^* of an emitted photon is provided as follows by Eq. (2.27) of Ref. 3:

$$A_\mu^* = (2\pi)^{-3/2} (2\omega)^{-1/2} e_\mu^* \times e^{-i\mathbf{k} \cdot [\mathbf{R} + (M_P/M)\mathbf{r}_P + (M_T/M)\mathbf{r}_T]}, \quad (2.2)$$

where \mathbf{k} , ω , and e_μ^* are the momentum, energy, and polarization vector of an emitted photon, respectively, \mathbf{R} is the position vector of the center of mass of the collision system, and \mathbf{r}_P and \mathbf{r}_T are the electronic coordinates with respect to P and T , respectively. Moreover, the masses of P , T , and e are defined as M_P , M_T , and m , respectively, and the reduced masses and the total mass of the system are given by $\lambda_P = M_P/(M_P + m)$, $\lambda_T = M_T/(M_T + m)$, and $M = M_P + M_T + m$. The final wave function $\Psi_f^{(-)}$ is provided by the framework of the RIA corresponding to Eq. (2.26) of Ref. 3 as

$$\Psi_f^{(-)} = (2\pi)^{-3/2} e^{i(\mathbf{K}_f + \mathbf{P}_f) \cdot \mathbf{R}} e^{i\lambda_P [M_P + m] \mathbf{K}_f - M_T \mathbf{P}_f \cdot (\mathbf{r}_P - \lambda_T \mathbf{r}_T) / M} \times \psi_{\mathbf{p}',+}^{(-)}(\mathbf{r}_T) \varphi_P(\mathbf{r}_P) u_P^{(f_P)}(\lambda_P \mathbf{P}_f) u_T^{(f_T)}(\mathbf{K}_f) u_e^{(f_e)}((1 - \lambda_P) \mathbf{P}_f). \quad (2.3)$$

Here, \mathbf{K}_f is the recoiling momentum of T and \mathbf{P}_f is the relative momentum of the composite system (P, e) with respect to T , respectively. $u_P^{(f_P)}$, $u_T^{(f_T)}$, and $u_e^{(f_e)}$ stand for free spinors of particles P , T , and e with their helicities f_P , f_T , and f_e , respectively. The arguments of spinors indicate the momenta of respective particles. φ_P is the 4×4 matrix associated with the wave function of the final bound electron and has the form

$$\varphi_P(\mathbf{r}_P) = N_P^{-1} [1 + \gamma_4 \gamma \cdot \nabla_{\mathbf{r}_P} / (2m)] \varphi_P^{(0)}(\mathbf{r}_P), \quad (2.4)$$

where $\varphi_P^{(0)}(\mathbf{r}_P)$ is a normalized solution of the Schrödinger equation for (P, e) at rest. The relativistic translational effect (the Lorentz contraction) of the atom (P, e) moving with \mathbf{P}_f with respect to T has been approximated as being incorporated in the spinors $u_P^{(f_P)}$ and $u_e^{(f_e)}$. N_P is a normalization constant for φ_P which is determined so as to satisfy

$$\langle \varphi_P u_e^{(f_e)} | \varphi_P u_e^{(f_e)} \rangle = 1.$$

(Even in the case of a hydrogenlike uranium, N_P amounts to no more than 1.05.) The second term of square brackets of Eq. (2.4) represents a relativistic Z_P correction to the nonrelativistic wave function. While we know the exact wave function for (P, e) satisfying the Dirac equation,

it is here replaced by the approximated one as Eq. (2.4) for a reason mentioned later. $\psi_{\mathbf{p}',+}^{(-)}(\mathbf{r}_T)$ of Eq. (2.3) is related with the relativistic outgoing Coulomb wave function mediated by the potential of T and e with the momentum \mathbf{p}' equal to $\lambda_T(1 - \lambda_P)\mathbf{P}_f - (1 - \lambda_T)\mathbf{K}_f$. It is given by³

$$\psi_{\mathbf{p}',+}^{(-)}(\mathbf{r}_T) = (2\pi)^{-3/2} N(\nu_T) e^{i\mathbf{p}' \cdot \mathbf{r}_T} \times [1 + \gamma_4 \gamma \cdot \nabla_{\mathbf{r}_T} / (2E_{\mathbf{p}'})] \times {}_1F_1(-i\nu_T, 1; -i(|\mathbf{p}'||\mathbf{r}_T| + \mathbf{p}' \cdot \mathbf{r}_T)), \quad (2.5)$$

where $E_{\mathbf{p}'} = (\mathbf{p}'^2 + m^2)^{1/2}$ and $N(\nu_T) = e^{\pi\nu_T/2} \Gamma(1 - i\nu_T)$ with $\nu_T = Z_T \alpha E_{\mathbf{p}'} / |\mathbf{p}'|$ (α is the fine structure constant). ${}_1F_1(\mu, \nu; z)$ and $\Gamma(z)$ denote the confluent hypergeometric function and the Γ function, respectively.

By following the assumption that the collision is quite asymmetric (i.e., $Z_P \gg Z_T$), the initial total wave function $\Psi_i^{(+)}$ of Eq. (2.1) becomes

$$\Psi_i^{(+)} = (1 + G_P^{(+)} V_P) \Phi_i, \quad (2.6)$$

where $G_P^{(+)}$ is a relativistic Green function incorporating an effect of a strong potential V_P between P and e to all orders and provided by

$$G_P^{(+)} = \left[E - \sum_{N=P,T,e} K_N - V_P + i\eta \right]^{-1}. \quad (2.7)$$

Here, K_N is a relativistic free Hamiltonian of a particle N and η an infinitesimal real positive value. Φ_i denotes the initial free wave function and has the expression

$$\begin{aligned} \Phi_i &= (2\pi)^{-3} e^{i(\mathbf{K}_i + \mathbf{P}_i) \cdot \mathbf{R}} \\ &\times e^{i[(M_T + m)\mathbf{K}_i - M_P \mathbf{P}_i] \cdot (\lambda_T \mathbf{r}_T - \mathbf{r}_P) / M} \\ &\times u_P^{(i_P)}(\mathbf{K}_i) u_T^{(i_T)}(\lambda_T \mathbf{P}_i) \varphi_T(\mathbf{r}_T) \\ &\times u_e^{(i_e)}((1 - \lambda_T) \mathbf{P}_i), \end{aligned} \quad (2.8)$$

where \mathbf{K}_i is the incident momentum of P and \mathbf{P}_i is the relative momentum of the composite system (T, e) with respect to P , respectively. Superscripts i_P , i_T , and i_e denote initial helicities of P , T , and e , respectively. The 4×4 matrix $\varphi_T(\mathbf{r}_T)$ related to the initial bound state is given correspondingly to Eq. (2.4) by

$$\varphi_T(\mathbf{r}_T) = N_T^{-1} [1 + \gamma_4 \gamma \cdot \nabla_{\mathbf{r}_T} / (2m)] \varphi_T^{(0)}(\mathbf{r}_T), \quad (2.9)$$

where $\varphi_T^{(0)}$ satisfies the Schrödinger equation for (T, e) and N_T is a normalization constant. The effect of the Lorentz contraction of (T, e) traveling with P_i with respect to P is included in the spinors of $u_P^{(i_P)}$ and $u_e^{(i_e)}$ as the same with the statement on Eq. (2.4).

Inserting in Eq. (2.6) the complete set $\{\chi\}$, given by

$$\chi = \prod_{N=P,T,e} (2\pi)^{-3/2} e^{i\mathbf{K}_N \cdot \mathbf{x}_N} w_N^{(n_N)}(\mathbf{K}_N), \quad (2.10)$$

$\Psi_i^{(+)}$ becomes

$$\Psi_i^{(+)} = \sum \psi^{(+)} \langle \chi | \Phi_i \rangle, \quad (2.11)$$

where the sum is over intermediate states. Here, \mathbf{K}_N is an intermediate momentum of a particle N and \mathbf{x}_N its position vector defined by

$$\mathbf{x}_P = \mathbf{R} + [M_T \mathbf{r}_T - (M_T + m) \mathbf{r}_P] / M,$$

$$\mathbf{x}_T = \mathbf{R} + [M_P \mathbf{r}_P - (M_P + m) \mathbf{r}_T] / M,$$

and

$$\mathbf{x}_e = \mathbf{R} + (M_P \mathbf{r}_P + M_T \mathbf{r}_T) / M,$$

respectively. A free spinor $w_e^{(n_e)}(\mathbf{K}_e)$ with a helicity n_e and a momentum \mathbf{K}_e is equal to $u_e^{(n_e)}(\mathbf{K}_e)$ for a positive energy state (an electron) and $v_e^{(n_e)}(\mathbf{K}_e)$ for a negative energy state (a positron), respectively. Spinors $w_P^{(n_P)}(\mathbf{K}_P)$ and $w_T^{(n_T)}(\mathbf{K}_T)$ are assumed equal to $u_P^{(n_P)}(\mathbf{K}_P)$ and $u_T^{(n_T)}(\mathbf{K}_T)$, respectively, because the contributions of antiparticles of P and T are completely negligible in the present intermediate states. A summation of Eq. (2.11) is taken with respect to all of the intermediate momentum \mathbf{K}_N , the helicity n_N , and the sign of the intermediate energy state. $\langle \chi | \Phi_i \rangle$ of Eq. (2.11) is given by

$$\begin{aligned} \langle \chi | \Phi_i \rangle &= \left[\prod_N w_N^{(n_N)}(\mathbf{K}_N) \right] u_P^{(i_P)}(\mathbf{K}_i) u_T^{(i_T)}(\lambda_T \mathbf{P}_i) \\ &\times \hat{\varphi}_T(\mathbf{q}) u_e^{(i_e)}((1 - \lambda_T) \mathbf{P}_i) \\ &\times \delta^{(3)}(\mathbf{K}_P - \mathbf{K}_i) \delta^{(3)}(\mathbf{K}_T + \mathbf{K}_e - \mathbf{P}_i), \end{aligned} \quad (2.12)$$

where $\hat{\varphi}_T(\mathbf{q})$ is the momentum-space wave function associated with $\varphi_T(\mathbf{r}_T)$ with $\mathbf{q} = \lambda_T \mathbf{K}_e - (1 - \lambda_T) \mathbf{K}_T$. Furthermore, the wave function $\psi^{(+)}$ is expressed as

$$\begin{aligned} \psi^{(+)} &= (2\pi)^{-3} e^{-i\{\mathbf{K}_T \cdot \mathbf{x}_T + (\mathbf{K}_P + \mathbf{K}_e) \cdot [\lambda_P \mathbf{x}_P + (1 - \lambda_P) \mathbf{x}_e]\}} \\ &\times u_P^{(n_P)}(\mathbf{K}_P) u_T^{(n_T)}(\mathbf{K}_T) \psi_{-p, \pm}^{(+)}(\mathbf{r}_P) w_e^{(n_e)}(\mathbf{K}_e), \end{aligned} \quad (2.13)$$

where $\psi_{-p, +}^{(+)}(\mathbf{r}_P)$ and $\psi_{-p, -}^{(+)}(\mathbf{r}_P)$ are matrices associated with the relativistic incoming Coulomb wave function of an intermediate electron and that of an intermediate positron with a momentum $-\mathbf{p}$ equal to $\lambda_P \mathbf{K}_e - (1 - \lambda_P) \mathbf{K}_P$. These are provided by

$$\begin{aligned} \psi_{-p, \pm}^{(+)}(\mathbf{r}_P) &= \{1 + [\pm E_p - (-i\boldsymbol{\alpha} \cdot \nabla_{\mathbf{r}_P} + m\beta + V_P) + i\eta]^{-1} V_p\} \\ &\times (2\pi)^{-3/2} e^{-i\mathbf{p} \cdot \mathbf{r}_P}, \end{aligned} \quad (2.14)$$

where an off-shell energy in the Green function has been replaced by the on-shell energy $\pm E_p$ with $E_p = (\mathbf{p}^2 + m^2)^{1/2}$ according to the framework of the IA. If the moving coordinate is chosen as a frame of reference, the potential V_P is nothing but the Coulomb potential without including a spin-orbit coupling as stated in Sec. I. (We will explicitly designate the choice of a projectile frame in Sec. III.) Thus Eq. (2.14) can be further reduced to the form¹³

$$\begin{aligned} \psi_{-p, \pm}^{(+)}(\mathbf{r}_P) &= (2\pi)^{-3/2} N(\pm \nu_P) e^{-i\mathbf{p} \cdot \mathbf{r}_P} \\ &\times [1 \pm \gamma_4 \gamma \cdot \nabla_{\mathbf{r}_P} / (2E_p)] \\ &\times {}_1F_1(\pm i\nu_P, 1; i(|\mathbf{p}||\mathbf{r}_P| + \mathbf{p} \cdot \mathbf{r}_P)), \end{aligned} \quad (2.15)$$

where $N(\pm \nu_P) = e^{\pm \pi \nu_P / 2} \Gamma(1 \pm i\nu_P)$ with $\nu_P = Z_P \alpha E_p / |\mathbf{p}|$. The relativistic pure Coulomb wave function satisfying $[\pm E_p - (-i\boldsymbol{\alpha} \cdot \nabla_{\mathbf{r}_P} + m\beta + V_P)] \tilde{\psi}_{-p, \pm}^{(+)}(\mathbf{r}_P) = 0$ cannot be obtained in a closed analytic form because of impossibility of separating this Dirac equation in the parabolic coordinates.¹⁴ Its exact expression is known only in the form of the infinite series with respect to partial waves but it is difficult to use for practical calculations. For this reason we have replaced $\tilde{\psi}_{-p, \pm}^{(+)}$ approximately by the wave function $\psi_{-p, \pm}^{(+)} w_e^{(n_e)}$. This type of the approximate wave function is called the Sommerfeld-Maue wave function.¹⁵ In addition, the relativistic discrete wave function $\varphi_P(\mathbf{r}_P)$ has been reduced into the form of Eq. (2.4) for the reason of retaining the same precision of approximations with that of $\psi_{-p, \pm}^{(+)}(\mathbf{r}_P)$.

Combining Eq. (2.11) with formulas from Eqs. (2.12)–(2.15) yields the RIA wave function as follows:

$$\begin{aligned}
\Psi_i^{(+)} = & (2\pi)^{-3/2} e^{i\lambda_T(\mathbf{K}_i + \mathbf{P}_i) \cdot \mathbf{R}} e^{i[(M_T + m)\mathbf{K}_i - M_P \mathbf{P}_i] \cdot (\mathbf{r}_T - \lambda_P \mathbf{r}_P) / M} \\
& \times [\psi_{-\mathbf{p},+}^{(+)}(\mathbf{r}_P) \Lambda_e^{(+)}((1 - \lambda_T)\mathbf{P}_i) + \psi_{-\mathbf{p},-}^{(+)}(\mathbf{r}_P) \Lambda_e^{(-)}((1 - \lambda_T)\mathbf{P}_i)] \\
& \times \varphi_T(\mathbf{r}_T) u_P^{(i_P)}(\mathbf{K}_i) u_T^{(i_T)}(\lambda_T \mathbf{P}_i) u_e^{(i_e)}((1 - \lambda_T)\mathbf{P}_i), \tag{2.16}
\end{aligned}$$

where $\Lambda_e^{(\pm)}(\mathbf{K})$ is an energy projection operator defined as

$$\Lambda_e^{(+)}(\mathbf{K}) = \sum_{n_e = \pm 1} u_e^{(n_e)}(\mathbf{K}) u_e^{(n_e)\dagger}(\mathbf{K})$$

and

$$\Lambda_e^{(-)}(\mathbf{K}) = \sum_{n_e = \pm 1} v_e^{(n_e)}(\mathbf{K}) v_e^{(n_e)\dagger}(\mathbf{K}).$$

In deriving Eq. (2.16), we have used the peaking approximation justified in the REC that contributions of a transferred momentum \mathbf{q} are neglected except for $\hat{\varphi}_T(\mathbf{q})$, a momentum-represented wave function of $\varphi_T(\mathbf{r}_T)$, on account of a sharp peak of an initial momentum distribution of a bound electron. The first and the second terms of square brackets of Eq. (2.16) indicate the effects of an electron and a positron propagating in the intermediate continuum states, respectively, as depicted in Fig. 1. In our previous paper,³ the intermediate positron contribution (the ICP effect) within the square brackets was neglected and the projection operator $\Lambda_e^{(+)}$ was set equal to unity. The presence of $\Lambda_e^{(\pm)}$ originates from $\{\chi\}$ of Eq. (2.10). Because $\Lambda_e^{(+)} + \Lambda_e^{(-)} = 1$, $\{\chi\}$ forms a complete set. In Eq. (2.7) of Ref. 3, however, $\{\chi_r\}$ does not include positron contributions, and hence it does not construct a complete set in principle. The difference between Eq. (2.25) of Ref. 3 and Eq. (2.16) above is attributed to such a situation.

III. CROSS SECTION AND LINEAR POLARIZATION CORRELATION OF AN EMITTED PHOTON

In this section, we derive an expression of a photon angular distribution for the K -REC with consideration of photon polarizations. The desired differential cross section is of the form

$$d\sigma/d\Omega_L = 2^{-1} (d\sigma/d\Omega_L)_{\text{unpol}} \left[1 + \sum_{i=1}^3 \xi_i P_i(\theta_L) \right], \tag{3.1}$$

where Ω_L is a solid angle associated with an emission angle θ_L of a photon in the laboratory frame, and a quantity $P_i(\theta_L)$ denotes a polarization correlation function of a photon satisfying $|P_i(\theta_L)| \leq 1$. $(d\sigma/d\Omega_L)_{\text{unpol}}$ stands for the differential cross section of an unpolarized emitted photon, i.e., the cross section that is averaged over with respect to polarization directions of photon and is weighted with the degree of freedom of photon polarizations by a factor of 2. Photon polarizations are described with three Stokes parameters ξ_i , $i = 1, 2, 3$, defined as¹⁶

$$\begin{aligned}
\xi_1 &= a_1^* a_1 - a_2^* a_2, \\
\xi_2 &= a_1 a_2^* + a_2 a_1^*, \\
\xi_3 &= i(a_1 a_2^* - a_2 a_1^*), \tag{3.2}
\end{aligned}$$

where a_1 represents a component of a photon polarization vector \mathbf{e} which is projected onto the scattering plane constructed by vectors of the incident velocity \mathbf{v} and the momentum \mathbf{k} of the emitted photon, a_2 stands for a component perpendicular to this plane along $\mathbf{k} \times \mathbf{v}$. Thus, $\mathbf{e} = a_1 \mathbf{e}^{(1)} + a_2 \mathbf{e}^{(2)}$ and $(\mathbf{e}^{(1)}, \mathbf{e}^{(2)}, \mathbf{k})$ form a right-hand set as depicted in Fig. 2, where $\mathbf{e}^{(1)}$ and $\mathbf{e}^{(2)}$ are unit vectors along the x and y axes, respectively, and hence \mathbf{k} is along the z axis. The parameter ξ_1 describes the linear polarization of the photon along the x or y axis. The parameter ξ_2 represents the linear polarization along directions rotated by $\pm\pi/4$ from the x axis. Finally, the parameter ξ_3 stands for the degree of circular polarization. For an unpolarized photon $\xi_1 = \xi_2 = \xi_3 = 0$, and for a completely polarized photon $\xi_1^2 + \xi_2^2 + \xi_3^2 = 1$.

In fact, the symmetrical invariance considerations¹⁷ permit only one nonvanishing polarization correlation, $P_1(\theta_L)$. Thus, the allowed polarization correlation of a REC photon represents only the effect of the linear polarized photon. Replacing $P_1(\theta_L)$ by $P(\theta_L)$, Eq. (3.1) becomes

$$d\sigma/d\Omega_L = 2^{-1} (d\sigma/d\Omega_L)_{\text{unpol}} [1 + P(\theta_L) \cos 2\phi], \tag{3.3}$$

where the polarization angle ϕ is an angle between the scattering plane (the x - z plane) and the polarization plane constructed by \mathbf{k} and \mathbf{e} . At this stage, \mathbf{e} has been written by $\mathbf{e} = e^{(1)} \cos\phi + e^{(2)} \sin\phi$ and then $\xi_1 = \cos 2\phi$.

Next, formulations are made for the differential cross section of the REC photons. At first, we calculate it in the moving frame (i.e., $\mathbf{P}_f = \mathbf{0}$) and finally Lorentz transform it into the laboratory frame (i.e., $\mathbf{P}_i = \mathbf{0}$). The photon angular distribution in the moving frame reads

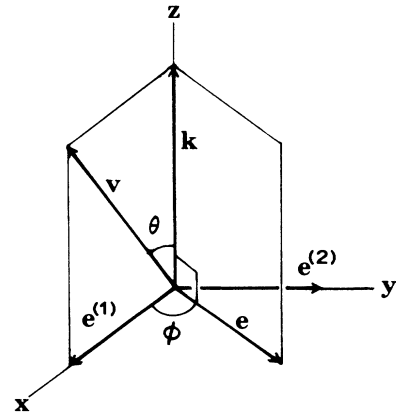


FIG. 2. Coordinate system for vectors \mathbf{k} , \mathbf{v} , and \mathbf{e} . The plane spanned by \mathbf{k} and \mathbf{v} is the scattering plane, and that by \mathbf{k} and \mathbf{e} is the polarization plane.

$$d\sigma/d\Omega_M = (2\pi)^4 |\mathbf{v}|^{-1} \times \sum \int d\omega_M \omega_M^2 \int d\mathbf{q} \langle |t^{\text{REC}}|^2 \rangle \times \delta(\omega_M - \omega_M^{(0)} - \gamma \mathbf{v} \cdot \mathbf{q}), \quad (3.4)$$

where $\omega_M^{(0)}$ indicates the peak position of the photon energy ω_M in the moving frame and is given by $\omega_M^{(0)} = m(\gamma \xi_T - \xi_P)$ with $\gamma = (1 - |\mathbf{v}|^2)^{-1/2}$, $\xi_P = [1 - (Z_P \alpha)^2]^{1/2}$, and $\xi_T = [1 - (\zeta_T \alpha)^2]^{1/2}$, with ζ_T being the optimized ζ exponent of an active electron. The summation is taken with respect to ζ_T values, i.e., initial states of bound electrons participating in the REC. Here θ_M is defined as an emission angle of a photon in the moving frame, and Ω_M is a solid angle associated with this. The last term in the energy-conserving δ function represents the Doppler-broadening effect of the REC photon spectrum. Moreover, t^{REC} and $\langle |t^{\text{REC}}|^2 \rangle$ have been defined as

$$T^{\text{REC}} = t^{\text{REC}} \delta^{(3)}(\mathbf{K}_i + \mathbf{P}_i - \mathbf{K}_f - \mathbf{k}) \quad (3.5)$$

and

$$\langle |t^{\text{REC}}|^2 \rangle = 8^{-1} \sum |t^{\text{REC}}|^2, \quad (3.6)$$

with the sum being over the helicities, where we have taken the average with respect to the initial helicities and the summation with respect to the final ones of all three particles P , T , and e .

Incorporating Eqs. (2.1)–(2.5), (2.16), and (3.5), we get

$$t^{\text{REC}} = -(2\omega_M)^{-1/2} (2\pi)^{-3/2} e u_P^{(f_P)\dagger}(\mathbf{0}) u_P^{(i_P)}(\mathbf{p} + \mathbf{k}) \times u_T^{(f_T)\dagger}(\lambda_T \mathbf{P}_i) u_T^{(i_T)}(\lambda_T \mathbf{P}_i) u_e^{(f_e)\dagger}(\mathbf{0}) \times e_\mu^* Q_\mu u_e^{(i_e)}(-\mathbf{p}), \quad (3.7)$$

where use has been made of kinematic relations of $\mathbf{K}_i = \mathbf{p} + \mathbf{k}$, $\mathbf{K}_f = \lambda_T \mathbf{P}_i$, $(1 - \lambda_T) \mathbf{P}_i = -\mathbf{p}$, and $\mathbf{p}' = \mathbf{p}$. Here, the relative velocity \mathbf{v} of the present system is given by $\mathbf{v} = -\mathbf{P}_i / [\mathbf{P}_i^2 + (M_T + m)^2]^{1/2}$ and then $\mathbf{p} \approx m\gamma \mathbf{v}$. The quantity Q_μ is defined as being equal to the sum of $Q_\mu^{(+)}$ and $Q_\mu^{(-)}$, which are defined by

$$Q_\mu^{(\pm)} = \int \int d\mathbf{r}_P d\mathbf{r}_T e^{-i\mathbf{k} \cdot \mathbf{r}_P} e^{iq \cdot \mathbf{r}_T} \varphi_P^\dagger(\mathbf{r}_P) \psi_{\mathbf{p}, \pm}^{(-)\dagger}(\mathbf{r}_T) \gamma_\mu \times \psi_{-\mathbf{p}, \pm}^{(+)}(\mathbf{r}_P) \Lambda_e^{(\pm)}(-\mathbf{p}) \varphi_T(\mathbf{r}_T). \quad (3.8)$$

$$I^{(2)}(\mathbf{p}, \mathbf{k}, \mathbf{q}) = [(1 - \gamma^{-1})/2][\mathbf{v} \cdot (\mathbf{U} + \mathbf{V})]/(1 - \gamma^{-1}) + 2(\mathbf{v} \cdot \mathbf{W}) - iX]^2 + [(1 + \gamma^{-1})/2][|\mathbf{U} + \mathbf{V}|^2 - |\mathbf{v} \cdot (\mathbf{U} + \mathbf{V})|/|\mathbf{v}|]^2. \quad (3.14)$$

\mathbf{U} , \mathbf{V} , \mathbf{W} , and X have been defined as $\mathbf{U} = \mathbf{B}_P^{(+)} A_T + A_P^{(+)} \mathbf{C}_T$, $\mathbf{V} = \mathbf{C}_P^{(+)} A_T + A_P^{(-)} \mathbf{B}_T$, $\mathbf{W} = (A_P^{(+)} - A_P^{(-)}) \mathbf{B}_T / 2$, and $X = A_P^{(+)} A_T$, respectively, where

$$A_P^{(\pm)} = (2\pi)^{-3/2} N(\pm v_P) \int d\mathbf{r}_P e^{-i(\mathbf{p} + \mathbf{k}) \cdot \mathbf{r}_P} \varphi_P^{(0)*}(\mathbf{r}_P) F^{(\pm)}(\mathbf{r}_P), \quad \mathbf{B}_P^{(+)} = (2m)^{-1} (2\pi)^{-3/2} N(v_P) \int d\mathbf{r}_P e^{-i(\mathbf{p} + \mathbf{k}) \cdot \mathbf{r}_P} [\nabla_{\mathbf{r}_P} \varphi_P^{(0)*}(\mathbf{r}_P)] F^{(+)}(\mathbf{r}_P), \quad \mathbf{C}_P^{(+)} = (2E_P)^{-1} (2\pi)^{-3/2} N(v_P) \int d\mathbf{r}_P e^{-i(\mathbf{p} + \mathbf{k}) \cdot \mathbf{r}_P} \varphi_P^{(0)*}(\mathbf{r}_P) [\nabla_{\mathbf{r}_P} F^{(+)}(\mathbf{r}_P)], \quad (3.15)$$

Effects of $Q_\mu^{(\pm)}$ to the REC are visualized as in Fig. 1. Especially, attention should be paid to $Q_\mu^{(-)}$ because it is related with the ICP effect.

By using Eq. (3.7), Eq. (3.6) becomes

$$\langle |t^{\text{REC}}|^2 \rangle = (2\pi)^{-2} \alpha \omega_M^{-1} \rho_{\mu\nu}^{(\gamma)} \times 2^{-1} \text{Tr}[\bar{\Lambda}_e^{(+)}(\mathbf{0}) Q_\mu \bar{\Lambda}_e^{(+)}(-\mathbf{p}) \bar{Q}_\nu], \quad (3.9)$$

where the fine-structure constant α has been defined in the Heaviside unit as $\alpha = e^2/(4\pi)$, $\bar{Q}_\nu = \gamma_4 Q_\nu^+ \gamma_4$, and $\bar{\Lambda}_e^{(+)}(\mathbf{K})$ is a Casimir operator defined as $\bar{\Lambda}_e^{(+)}(\mathbf{K}) = \Lambda_e^{(+)}(\mathbf{K}) \gamma_4$. In Eq. (3.9), we have neglected effects of the nuclear spinors $u_P^{(i_P)}$, $u_P^{(f_P)}$, $u_T^{(i_T)}$, and $u_T^{(f_T)}$ because they contribute to Eq. (3.9) by a factor comparable to the order of unity. A density matrix $\rho_{\mu\nu}^{(\gamma)}$ for a photon polarization is given by¹⁵

$$\rho_{\mu\nu}^{(\gamma)} = e_\mu^* e_\nu = \sum_{a,b=1}^2 \rho_{ab} e_\mu^{(a)} e_\nu^{(b)}. \quad (3.10)$$

Here ρ_{ab} is a photon polarization tensor defined by

$$\rho_{ab} = \frac{1}{2} \begin{bmatrix} 1 + \xi_1 & \xi_2 - i\xi_3 \\ \xi_2 + i\xi_3 & 1 - \xi_1 \end{bmatrix} \quad (3.11)$$

and $e_\lambda^{(i)} = (\mathbf{e}^{(i)}, 0)$ for $i = 1, 2$ and $\lambda = \mu, \nu$.

After lengthy and complicated calculations of the trace in Eq. (3.9), we obtain

$$\langle |t^{\text{REC}}|^2 \rangle = (2\pi)^{-2} \alpha \omega_M^{-1} [(1 + \xi_1) I^{(1)}(\mathbf{p}, \mathbf{k}, \mathbf{q})/2 + I^{(2)}(\mathbf{p}, \mathbf{k}, \mathbf{q})]. \quad (3.12)$$

We have expanded Q_μ with respect to $\nabla_{\mathbf{r}_P}/(2E_P)$, $\nabla_{\mathbf{r}_P}/(2m)$, $\nabla_{\mathbf{r}_T}/(2E_P)$, and $\nabla_{\mathbf{r}_T}/(2m)$ up to the first order to evaluate Eq. (3.9) into the form of Eq. (3.12). Here,

$$I^{(1)}(\mathbf{p}, \mathbf{k}, \mathbf{q}) = -2(1 + \gamma^{-1}) \text{Re}[(\mathbf{e}^{(1)} \cdot \mathbf{U})^* (\mathbf{e}^{(1)} \cdot \mathbf{V})] - 4 \text{Re}[(\mathbf{e}^{(1)} \cdot \mathbf{U})^* (\mathbf{v} \cdot \mathbf{W})] (\mathbf{e}^{(1)} \cdot \mathbf{v}) - 2 \text{Im}[(\mathbf{e}^{(1)} \cdot \mathbf{U})^* X] (\mathbf{e}^{(1)} \cdot \mathbf{v}) \quad (3.13)$$

and

and

$$\begin{aligned}
 A_T &= (2\pi)^{-3/2} N(\nu_T) \int d\mathbf{r}_T e^{i\mathbf{q}\cdot\mathbf{r}_T} \varphi_T^{(0)}(\mathbf{r}_T) F(\mathbf{r}_T), \\
 B_T &= (2m)^{-1} (2\pi)^{-3/2} N(\nu_T) \\
 &\quad \times \int d\mathbf{r}_T e^{i\mathbf{q}\cdot\mathbf{r}_T} [\nabla_{\mathbf{r}_T} \varphi_T^{(0)}(\mathbf{r}_T)] F(\mathbf{r}_T), \\
 C_T &= (2E_p)^{-1} (2\pi)^{-3/2} N(\nu_T) \\
 &\quad \times \int d\mathbf{r}_T e^{i\mathbf{q}\cdot\mathbf{r}_T} \varphi_T^{(0)}(\mathbf{r}_T) [\nabla_{\mathbf{r}_T} F(\mathbf{r}_T)].
 \end{aligned} \tag{3.16}$$

In Eq. (3.15), $A_p^{(+)}$, $B_p^{(+)}$, and $C_p^{(+)}$ denote contributions of an intermediate electron, and $A_p^{(-)}$ represents an effect of an intermediate positron. We have used the abbreviations for the hypergeometric functions that

$$F^{(\pm)}(\mathbf{r}_p) = {}_1F_1(\pm i\nu_p, 1; i(|\mathbf{p}||\mathbf{r}_p| + \mathbf{p}\cdot\mathbf{r}_p))$$

and

$$F(\mathbf{r}_T) = {}_1F_1(i\nu_T, 1; i(|\mathbf{p}||\mathbf{r}_T| + \mathbf{p}\cdot\mathbf{r}_T)).$$

Integrations of Eqs. (3.15) and (3.16) are performed by using the Nordsieck integrals.^{3,18} In Eq. (3.13), $\text{Re}[\dots]$ and $\text{Im}[\dots]$ denote real and imaginary parts of $[\dots]$, respectively. Furthermore, in obtaining Eqs. (3.13) and (3.14), we have employed the fact that the vectors \mathbf{U} , \mathbf{V} , and \mathbf{W} lie on the scattering plane of Fig. 2 and then $(\mathbf{e}^{(2)}\cdot\mathbf{U}) = (\mathbf{e}^{(2)}\cdot\mathbf{V}) = (\mathbf{e}^{(2)}\cdot\mathbf{W}) = 0$. At the sight of Eq. (3.12), it is found that there are no terms proportional to the Stokes parameters ξ_2 and ξ_3 . This property leads Eq. (3.4) to the same form with Eq. (3.3), except that the former is defined in the moving frame and the latter in the laboratory frame.

Inserting Eq. (3.12) into Eq. (3.4) and utilizing the Lorentz transformations,

$$\begin{aligned}
 \sin\theta_M &= \gamma^{-1} \sin\theta_L / (1 - |\mathbf{v}|\cos\theta_L), \\
 \cos\theta_M &= (\cos\theta_L - |\mathbf{v}|) / (1 - |\mathbf{v}|\cos\theta_L),
 \end{aligned} \tag{3.17}$$

and

$$d\sigma/d\Omega_L = (1 - \mathbf{v}^2)(1 - |\mathbf{v}|\cos\theta_L)^{-2} (d\sigma/d\Omega_M), \tag{3.18}$$

we get the photon angular distribution in the laboratory frame,

$$\begin{aligned}
 d\sigma/d\Omega_L &= (2\pi)^2 \alpha |\mathbf{v}|^{-1} (1 - \mathbf{v}^2) (1 - |\mathbf{v}|\cos\theta_L)^{-2} \\
 &\quad \times \langle\langle (1 + \cos 2\phi) I^{(1)}(\mathbf{p}, \mathbf{k}, \mathbf{q}) / 2 \\
 &\quad + I^{(2)}(\mathbf{p}, \mathbf{k}, \mathbf{q}) \rangle\rangle,
 \end{aligned} \tag{3.19}$$

where the symbol $\langle\langle \dots \rangle\rangle$ has been defined by the integrations

$$\langle\langle \dots \rangle\rangle = \sum \int d\omega_M \omega_M \int d\mathbf{q} \delta(\omega_M - \omega_M^{(0)} - \gamma\mathbf{v}\cdot\mathbf{q}) \dots, \tag{3.20}$$

where the sum is over the initial electron states. Here, we must replace the peak position of photon energy $\omega_M^{(0)}$ in the moving frame by that in the laboratory frame given by $\omega_L^{(0)} = \gamma^{-1} (1 - |\mathbf{v}|\cos\theta_L)^{-1} \omega_M^{(0)}$. The peaking approximation with respect to $|\hat{\varphi}_T(\mathbf{q})|^2$ is used for evaluation of the integral of Eq. (3.20). Comparing the resultant

differential cross section of Eq. (3.19) with Eq. (3.3), the angular distribution for unpolarized emitted photons and the linear polarization correlation of REC photons are obtained as

$$\begin{aligned}
 (d\sigma/d\Omega_L)_{\text{unpol}} &= (2\pi)^2 \alpha |\mathbf{v}|^{-1} (1 - \mathbf{v}^2) (1 - |\mathbf{v}|\cos\theta_L)^{-2} \\
 &\quad \times \langle\langle I^{(1)}(\mathbf{p}, \mathbf{k}, \mathbf{q}) + 2I^{(2)}(\mathbf{p}, \mathbf{k}, \mathbf{q}) \rangle\rangle,
 \end{aligned} \tag{3.21}$$

and

$$P(\theta_L) = \langle\langle I^{(1)}(\mathbf{p}, \mathbf{k}, \mathbf{q}) \rangle\rangle / \langle\langle I^{(1)}(\mathbf{p}, \mathbf{k}, \mathbf{q}) + 2I^{(2)}(\mathbf{p}, \mathbf{k}, \mathbf{q}) \rangle\rangle. \tag{3.22}$$

If a term $A_p^{(-)}$ is dropped in $I^{(1)}$ and $I^{(2)}$ of Eq. (3.21), this result corresponds to the expression of a cross section of Ref. 3. It is easily shown that by taking the limit of the relativistic Born approximation, i.e., $\nu_p, \nu_T \rightarrow 0$, leads Eqs. (3.21) and (3.22) to just the same with the Sauter formula¹⁹ for unpolarized REC photons and the expressions of Eq. (9) of Ref. 4, respectively.

IV. RESULTS AND DISCUSSION

A. Total cross section

Total cross sections have been calculated by integrating Eq. (3.21) with respect to the solid angle Ω_L . They include all of the relativistic effects explained in Sec. I: the relativistic velocity effect, the high- Z_p effect, the spin-orbit coupling, and the ICP effect. Especially, pay attention to the last new effect. K -REC cross sections for collision systems of Xe^{54+} -Be and U^{92+} -Be are shown in Figs. 3 and 4, respectively. In practical calculations, we have used the Slater rule to estimate optimized ξ exponents ξ_T of Be electrons as 3.7 for the 1s state and 0.975 for the 2s-state. Both Figs. 3 and 4 contain two theoretical curves: one is the result by the RIA with consideration of the ICP, i.e., in accordance with both of graphs of Fig. 1, and the other by the RIA irrespective of the ICP effect, i.e., with considering only the first diagram of Fig. 1. The differences of the respective two curves indicate magnitudes of the ICP effect to the K -REC. In Table I we show the degree of the ICP with respect to electric charges of projectiles as well as velocities.

The ICP has little effect on the cross section of the Ne^{10+} -Be system over all velocity regions. In contrast with this, the U^{92+} -Be system is much influenced with the ICP, above all, on the occasion of high-impact velocities. At the velocity of 0.99, this effect gives no less than 2.4 times greater contributions in comparison with the results without consideration of the ICP. As stated in Sec. I, the ICP is physically interpreted as an effect based on the breakup of virtual e^+e^- pairs (vacuum polarization cloud around a projectile ion induced by the presence of its strong electric fields) into real pairs due to the projectile motion. Thus we come to the conclusion that as long as a projectile charge is very large, an intermediate positron has nearly the same degree of contributions to the K -REC with that of an associated electron. The velocity

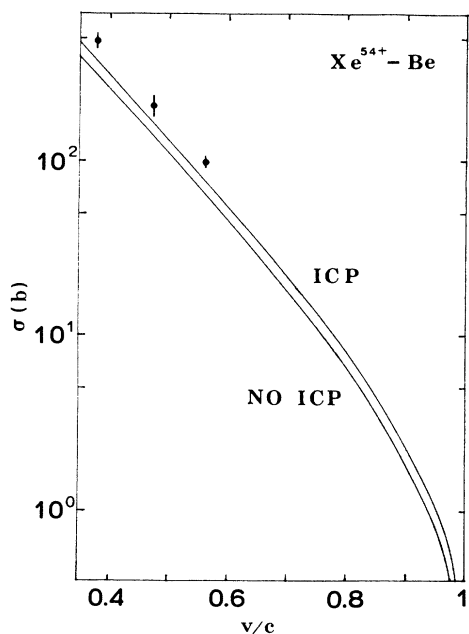


FIG. 3. REC total cross sections for a Xe^{54+} -Be collision system. ICP and no ICP mean RIA calculations with and without including the internal conversion process, respectively. Experimental values are cited from W. E. Meyerhof, R. Anholt, J. Eichler, H. Gould, Ch. Munger, J. Alonso, P. Thieberger, and H. E. Wegner, Phys. Rev. A 32, 3291 (1985).

dependence of the ICP is less pronounced than expected at the outset. For relativistic heavy ion-atom collisions, not to speak of the present REC, in general, it might be improper to neglect the effects of the ICP fully from the

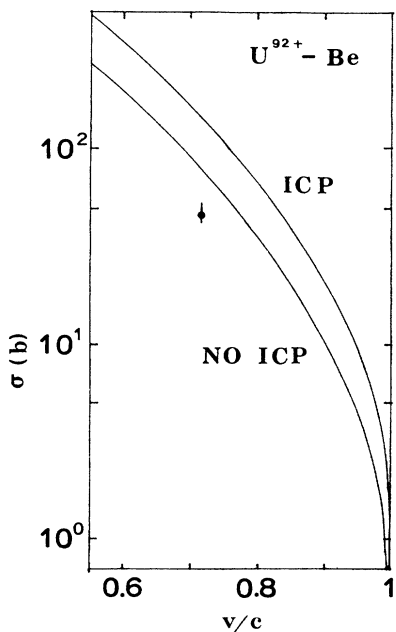


FIG. 4. Same as Fig. 3 except for a U^{92+} -Be collision system. The experimental value is quoted from Ref. 2.

TABLE I. Ratios of K -REC total cross sections calculated by using the RIA with incorporating effects of the ICP to cross sections by the RIA without the ICP. Numbers in parentheses denote digits of the third decimal.

Collision system	Incident velocity $ \mathbf{v} $			
	0.70	0.80	0.90	0.99
Ne^{10+} -Be	1.00(6)	1.00(7)	1.00(8)	1.00(9)
Xe^{54+} -Be	1.21	1.22	1.25	1.32
U^{92+} -Be	1.82	1.90	2.02	2.40

beginning as, for example, in the discussion of our preceding article.³

We are somewhat concerned with a simple velocity dependence of a REC total cross section. In the nonrelativistic energy region, as indicated by Briggs and Dettmann,²⁰ this is proportional to $|\mathbf{v}|^{-5}$. It is difficult to deduce such a simple rule from the present RIA method because a total cross section by this method is given numerically and is dependent on terms providing the ICP and the Z_P effects in complicated manners. Then, for simplicity, we evaluate a simple dependence of velocity by applying a least-square method to some calculated values at velocities $|\mathbf{v}|$ ranging from 0.1 to 0.8 for Ne^{10+} -Be, from 0.4 to 0.8 for Xe^{54+} -Be, and from 0.6 to 0.8 for U^{92+} -Be, respectively. In these velocity regions, logarithmically scaled cross sections show almost straight slopes as in Figs. 3 and 4. As a result, a semiempirical rule is obtained as $|\mathbf{v}|^{-p}$ with p equal to 4.98, 5.19, and 5.59 for respective collision systems. A slope of a total cross section with respect to ultrarelativistic velocities is steeper than that in the relativistic velocity region considered above.

Next, we evaluate the number of "available" target electrons² participating in the REC process. In accordance with the model of the quasifree target electrons, this effective number is approximated as Z_T . In other words, calculations for a valence electron yield the same cross section as for an inner-shell electron. Here, a discussion will be made on the criterion for the validity of the quasifree target electron model. From Eq. (3.20) by employing the peaking approximation, we get

$$\langle \cdots \rangle \approx N_{\text{eff}} \omega_{M,\text{val}}^{(0)} \int d\mathbf{q} \cdots, \quad (4.1)$$

where $\omega_{M,\text{val}}^{(0)}$ is the peak energy of a photon associated with a target valence electron and the effective number N_{eff} of electrons has been defined as

$$N_{\text{eff}} = \sum (\gamma \xi_T - \xi_P) / (\gamma \xi_{T,\text{val}} - \xi_P). \quad (4.2)$$

$\xi_{T,\text{val}}$ stands for $[1 - (\xi_{T,\text{val}} \alpha)^2]^{1/2}$ with $\xi_{T,\text{val}}$ being the ξ exponent of a valence electron and the summation is taken with respect to all of the active electron states satisfying the restriction

$$\gamma \xi_T \gtrsim \xi_P. \quad (4.3)$$

In deriving Eq. (4.2), the ξ_T dependence of the integrand \cdots of Eq. (4.1) is neglected for simplicity.

Letting the cross section from a valence electron be σ_{val} , then we obtain the expression

$$\sigma \approx N_{\text{eff}} \sigma_{\text{val}}. \quad (4.4)$$

The restriction of Eq. (4.3) reads

$$\xi_T \lesssim Z_P (\gamma^{-2} + v_P^{-2})^{1/2}, \quad (4.5)$$

where the argument of a square root is always greater than unity. Thus, as long as $\xi_T \lesssim Z_P$, all of the target electrons take part in the REC. Furthermore, if $Z_T \alpha \ll 1$, i.e., $\xi_T \approx 1$, N_{eff} is nearly equal to Z_T . As a result, the criteria for the validity of the quasifree target electron model become $\xi_T \lesssim Z_P$ and $Z_T \alpha \ll 1$. In the case of Xe^{54+} - and U^{92+} -Be system, the criteria hold true, and hence $N_{\text{eff}} \approx 4$ is obtained. However, in the case of the near symmetric collisions, e.g., U^{92+} -Ta, this criteria is partially broken down and N_{eff} is somewhat reduced from Z_T . The latter case might be important for calculations of charge equilibrium states of relativistic heavy ions passing through high- Z_T matter.²¹

Finally, we mention to comparisons of theoretical results with experimental values cited in Figs. 3 and 4. For a Xe^{54+} -Be system, the present calculation reproduces the experimental values fairly well. Thus, it is thought that the ICP effect can compensate to some extent discrepancies of the experimental results with the calculations neglecting the ICP effects.²² For a U^{92+} -Be system, however, the theoretical prediction is too high compared to the experiment. This disagreement might originate from the employment of the Sommerfeld-Maue wave function [Eq. (2.15)] instead of the exact relativistic Coulomb wave function. The Sommerfeld-Maue wave function holds correctly only in the high-energy domain and for a projectile charge satisfying $Z_P \alpha \ll 1$. Thus, the

full employment of the exact Coulomb wave function might reduce the theoretical result of Fig. 4 to some degree. Further comparisons are not thought to be worthwhile because there are little experimental data on the relativistic REC at the present time except for those cited here.

B. Photon angular distribution

We show normalized photon angular distributions $\sigma_N(\theta_L, \phi)$ at the polarization angles $\phi = 0^\circ$, 45° , and 90° for a Ne^{10+} -Be system in Fig. 5 and for a U^{92+} -Be system in Fig. 6, respectively. They are normalized by respective maximum values and given as follows by using Eq. (3.19):

$$\sigma_N(\theta_L, \phi = 0^\circ) \propto (1 - |\mathbf{v}| \cos \theta_L)^{-2} (K^{(1)} + K^{(2)}), \quad (4.6)$$

$$\sigma_N(\theta_L, \phi = 45^\circ) \propto (1 - |\mathbf{v}| \cos \theta_L)^{-2} (K^{(1)}/2 + K^{(2)}), \quad (4.7)$$

$$\sigma_N(\theta_L, \phi = 90^\circ) \propto (1 - |\mathbf{v}| \cos \theta_L)^{-2} K^{(2)}, \quad (4.8)$$

where $K^{(1)}$ and $K^{(2)}$ stand for $\langle\langle I^{(1)}(\mathbf{p}, \mathbf{k}, \mathbf{q}) \rangle\rangle$ and $\langle\langle I^{(2)}(\mathbf{p}, \mathbf{k}, \mathbf{q}) \rangle\rangle$, defined as Eqs. (3.13), (3.14), and (3.20). Maximum values normalizing respective cross sections are designated in Table II. A normalized photon angular distribution at $\phi = 45^\circ$ is the same with that for unpolarized emitted photons [see Eq. (3.21)] because $\xi_1 = 0$.

Firstly, we take the cross sections at $\phi = 45^\circ$ in Fig. 5 into consideration. Photons induced by collisions of Ne^{10+} on Be distribute symmetrically as $\sin^2 \theta_L$ at the incident energy up to 1 GeV/u ($|\mathbf{v}| = 0.87$). This is mainly due to the cancellation between a photon-retardation effect and an aberration effect as referred to in Sec. I. As

TABLE II. Maximum values (in units of barns) of photon angular distributions for collisions of (a) Ne^{10+} and (b) U^{92+} ions on Be atoms. Absolute photon angular distributions are obtained by multiplying normalized values of Figs. 3 and 4 by these quantities. Numbers (in units of degrees) within parentheses mean the associated emission angles of photons. Numbers in square brackets denote powers of ten.

(a) Ne^{10+} -Be				
Polarization angle (deg)	Incident energy (GeV/u)			
	0.1	1	10	100
0	0.984[-2] (91)	0.453[-4] (93)	0.132[-5] (36)	0.162[-6] (8)
45	0.494[-2] (91)	0.261[-4] (90)	0.142[-5] (27)	0.163[-6] (8)
90	0.284[-4] (77)	0.960[-5] (54)	0.153[-5] (23)	0.165[-6] (8)
(b) U^{92+} -Be				
Polarization angle (deg)	Incident energy (GeV/u)			
	0.5	1	10	100
0	0.276[+1] (93)	0.740[0] (93)	0.209[-1] (27)	0.252[-2] (7)
45	0.143[+1] (92)	0.410[-0] (91)	0.227[-1] (22)	0.255[-2] (7)
90	0.166[0] (180)	0.138[0] (45)	0.247[0] (20)	0.258[-2] (7)

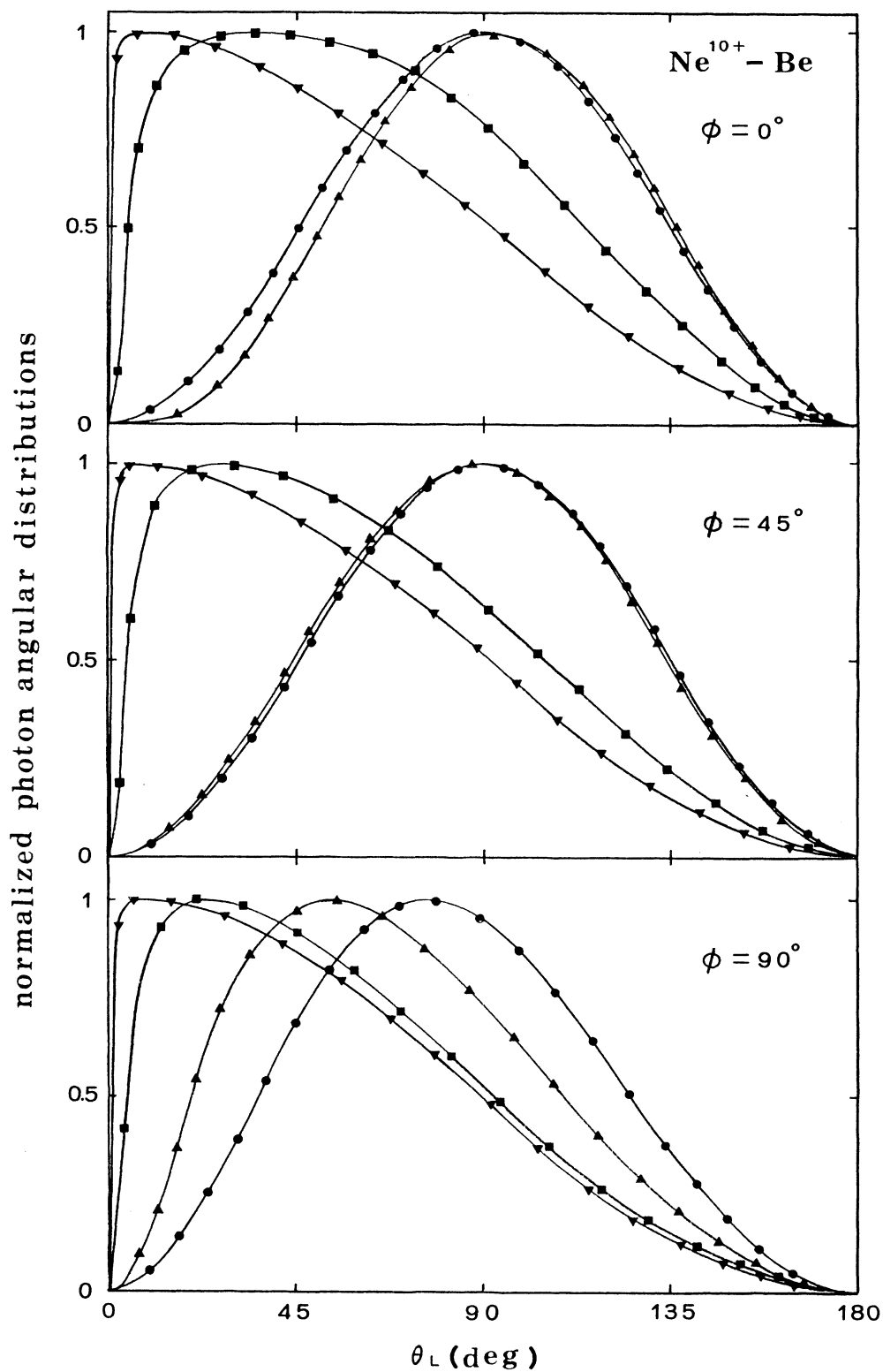


FIG. 5. Normalized photon angular distributions of K -REC induced by collisions of a Ne^{10+} ion on a Be atom. ϕ means the polarization angle of an emitted photon. \bullet , incident energy 0.1 GeV/ u ; \blacktriangle , 1 GeV/ u ; \blacksquare , 10 GeV/ u ; \blacktriangledown , 100 GeV/ u ; respectively.

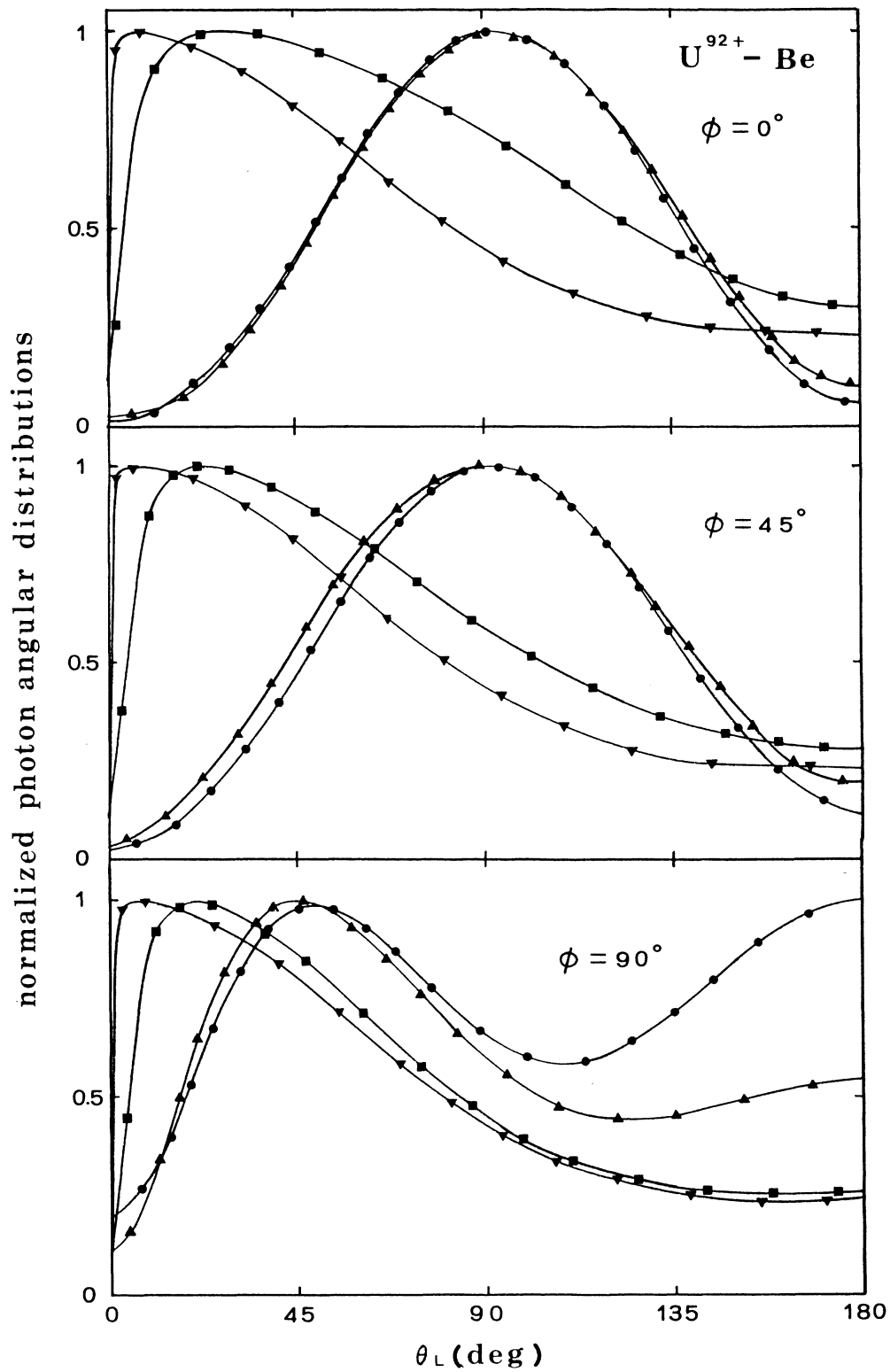


FIG. 6. Same as Fig. 5 except for a U^{92+} -Be collision system. Here, the curves \bullet represent the theoretical results at an incident energy 0.5 GeV/u.

the energy becomes larger, however, the radiation pattern comes to exhibit asymmetry. Such a tendency means the breakdown of this cancellation effect. At the ultrarelativistic energy of 100 GeV/ u ($|\mathbf{v}|=1$), the photon angular distribution gets to follow $\cos^2(\theta_L/2)$.²³ This behavior is much different from the conventional $\sin^2\theta_L$ dependence. This $\cos^2(\theta_L/2)$ dependence is ascribable to an ultrarelativistic effect that an electron moving at semilight velocity mainly emits photons in the forward direction relative to its trajectory. In the case of U^{92+} ion bombardments shown in Fig. 6, the radiation patterns are roughly the same with those induced by Ne^{10+} ion bombardments, and also indicate asymmetrical photon distributions in the ultrarelativistic energy domain. A remarkable feature of a U^{92+} -Be system is that a photon angular distribution is slightly enhanced in the backward direction relative to 90° in comparison with that of a Ne^{10+} -Be system. This enhancement does not vanish even if the relative velocity approaches light velocity. It is mainly because of a strong Coulomb distortion effect between a U^{92+} ion and an active electron as mentioned in Sec. I. A Coulomb distortion effect is evaluated by a parameter $\nu_p = Z_p\alpha/|\mathbf{v}|$ [see the statement below Eq. (2.15)]. At the velocity of light, this amounts to no less than $\nu_p=0.67$ and hence the strong distortion effect still survives. Moreover, it is thought that a relativistic high- Z_p effect of a K electron finally captured on a U^{92+} ion also partially contributes to the backward deviations of the photon angular distributions.

Radiation patterns at $\phi=0^\circ$ for both collision systems are almost the same with those at $\phi=45^\circ$. On the contrary, photon angular distributions at $\phi=90^\circ$ exhibit quite different radiation patterns from the above two. As shown in Eq. (4.8), distributions of photons at $\phi=90^\circ$ are determined only by a quantity $K^{(2)}$. In the ultrarelativistic velocity region, this predominates a quantity $K^{(1)}$ and provides the $\cos^2(\theta_L/2)$ dependence. On the other hand, $K^{(1)}$ is effective to a K -REC cross section only up to $|\mathbf{v}|$ below 0.8. Radiation patterns of a U^{92+} -Be system at $\phi=90^\circ$ are discriminated from those of a Ne^{10+} -Be system. This discrepancy is also due to high- Z_p effect of a projectile. Especially, the curves for a U^{92+} -Be system at incident energies 0.5 and 1 GeV/ u indicate the maximum values at $\theta_L=49^\circ$ and 45° and the minimum values at $\theta_L=109^\circ$ and 124° , respectively. Such a feature is absent in a Ne^{10+} -Be system.

In the case of a bombardment of a U^{92+} ion on a Be atom, the ICP have nearly the same degree of contribution to an absolute value of a photon angular distribution with that to a total cross section in Table I. However, there is little ICP effect to a normalized photon angular distribution even if an incident velocity is nearly equal to unity. An order of its effect is no more than 0.1–1.0 %.

C. Linear polarization correlation of an emitted photon

It is possible that a direction of a photon polarization vector \mathbf{e} varies in the relativistic velocity region, while it mostly remains lying on the scattering plane in the nonrelativistic velocity region. This nature is reflected by a

linear polarization correlation function $P(\theta_L)$ defined in Eq. (3.22). According to Eq. (3.3), this is rewritten as

$$P(\theta_L) = [(d\sigma/d\Omega_L)_{\phi=0^\circ} - (d\sigma/d\Omega_L)_{\phi=90^\circ}] / (d\sigma/d\Omega_L)_{\text{unpol}}. \quad (4.9)$$

Utilizing expressions of Eqs. (3.19) and (3.22), we can show that $P(\theta_L)=1$, 0, and -1 mean $(d\sigma/d\Omega_L) = A(\theta_L)K^{(1)}(1+\cos 2\phi)/2$, $A(\theta_L)K^{(2)}$, and $A(\theta_L)K^{(2)}(1-\cos 2\phi)/2$, respectively, with $A(\theta_L) = (2\pi)^2\alpha|\mathbf{v}|^{-1}(1-\mathbf{v}^2)(1-|\mathbf{v}|\cos\theta_L)^{-2}$. Thus, \mathbf{e} predominantly lies on the scattering plane spanned by \mathbf{k} and \mathbf{v} for $P(\theta_L)=1$ and mostly turns to the direction perpendicular to this plane for $P(\theta_L)=-1$. (See Fig. 2.) It is possible that \mathbf{e} points to all polarization directions with just the same rate as for $P(\theta_L)=0$.

For an impact of a projectile ion moving with a nonrelativistic velocity or an intermediate relativistic velocity (below 0.6), a direction of \mathbf{e} predominantly remains frozen onto the scattering plane, that is to say, $P(\theta_L)=1$ at all emission angles except for $\theta_L=0^\circ$ and 180° . With increasing incident velocity, the polarization vector is gradually changing its direction from on the scattering plane. At both the forward angle ($\theta_L=0^\circ$) and the backward angle ($\theta_L=180^\circ$), the polarization correlation should be zero for all impact velocities. (This requirement is not satisfied by a polarization correlation given by the relativistic Born approximation.⁴) From the physical point of view, this zero behavior is interpreted as follows: The scattering plane is formed by two vectors \mathbf{v} and \mathbf{k} and the emission angle of photons is defined as the angle between the two. Thus, the scattering plane cannot be uniquely defined in the case that \mathbf{v} and \mathbf{k} are parallel ($\theta_L=0^\circ$) and antiparallel ($\theta_L=180^\circ$), respectively. At these angles, it is possible that the polarization vector turns to all directions and hence the polarization correlation must become averaged to zero. This is because $P(0^\circ)=P(180^\circ)=0$.

In Fig. 7, we show the linear polarization correlations of REC photons induced by collisions of Ar^{18+} , Xe^{54+} , and U^{92+} on a Be atom for several relativistic velocities ranging from 0.7 (376 MeV/ u) to 0.99 (5.72 GeV/ u). For collisions of Ar^{18+} on Be, it is expected that the Born prediction holds true except for the forward and the backward angles. In this collision system, it is found that the crossover features appear for velocities above 0.8 and the crossover angle, at which a sign of a polarization correlation is changed, become larger with increasing velocity. Following the Born prediction,⁴ the crossover angle finally reaches 60° at the velocity of light. The polarization correlation tends to be flat, that is, $P(\theta_L)=0$ for all emission angles in the ultrarelativistic velocity region.

The tendency of $P(\theta_L)$ for Ar^{18+} ion impacts also applies on the whole to the cases for Xe^{54+} and U^{92+} ion impacts. Comparing these three cases, the respective polarization correlations exhibit nearly the same dependence on emission angles from 40° to 120° . In this region of an emission angle, high- Z_p effects of heavy ions have little influences on polarization correlations. Thus, the Born approximation is almost valid in spite of heavy ion-

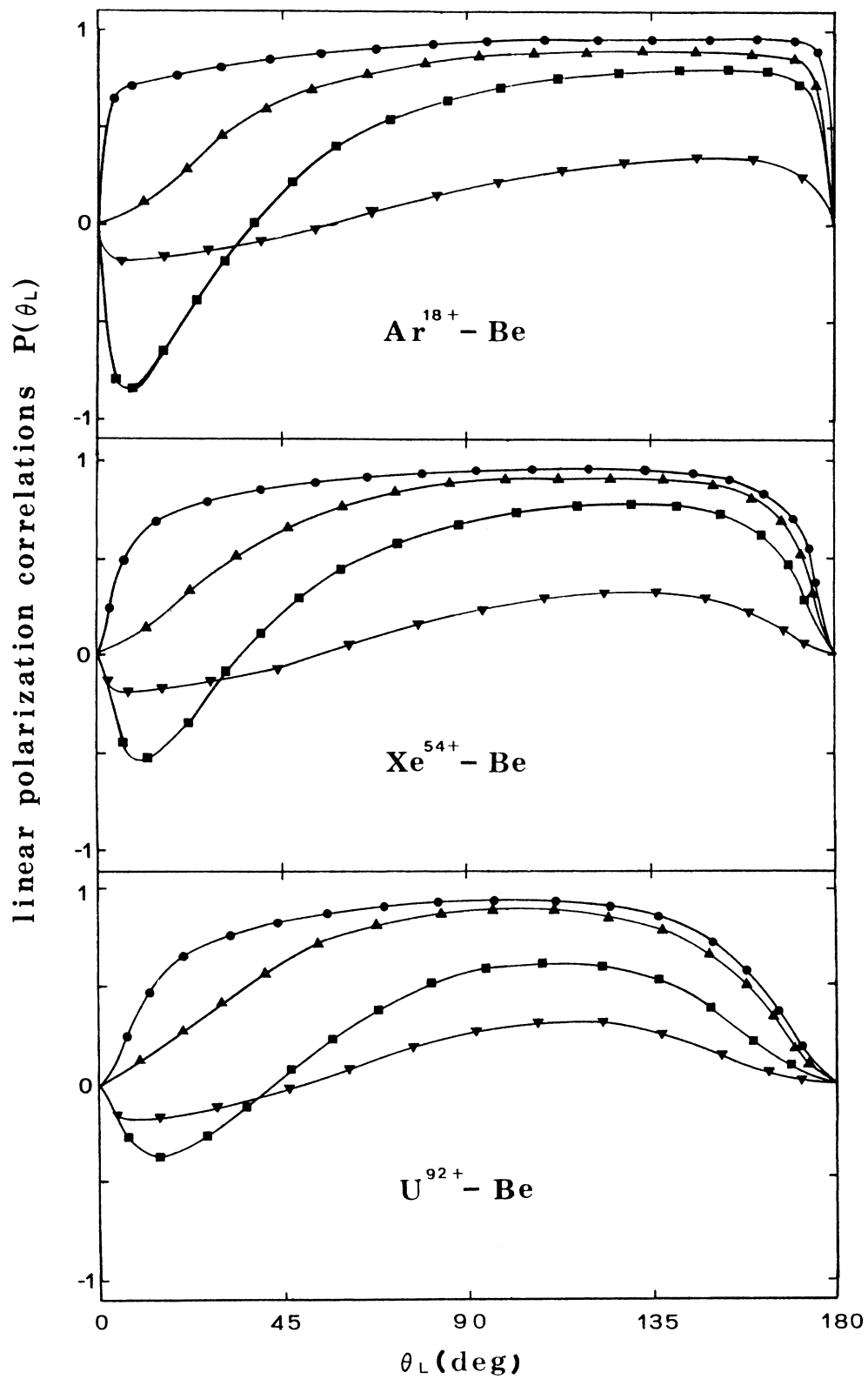


FIG. 7. Linear polarization correlations for K -REC photons induced by collisions of Ar^{18+} , Xe^{54+} , and U^{92+} ions on a Be atom. ●, the incident velocity in the unit of the light velocity 0.7; ▲, 0.8; ■, 0.9; ▼, 0.99; respectively.

TABLE III. Crossover angles (in units of degrees) of linear polarization correlations of K -REC photons induced by collisions of several projectile ions (Ne^{10+} , Ar^{18+} , Kr^{36+} , Xe^{54+} , Ta^{73+} , and U^{92+}) on Be atoms.

Incident velocity $ \mathbf{v} $	Projectile ions					
	Ne^{10+}	Ar^{18+}	Kr^{36+}	Xe^{54+}	Ta^{73+}	U^{92+}
0.85	26	26	25	24	22	20
0.90	37	37	36	35	34	32
0.95	46	46	45	44	43	41
0.99	55	55	54	53	51	49

atom collisions. Nevertheless, this simple prediction is destroyed in the vicinity of the angles at 0° and 180° . At these angles, high- Z_p effects play significant roles to determine a direction of a photon polarization vector.

Finally, we consider a Z_p dependence of a crossover angle, which is shown in Table III. Contrary to the first expectation, a crossover angle varies just slightly with increasing Z_p . Hence, the Born prediction holds approximately true for all projectile element.

V. CONCLUSIONS

We enumerate the conclusions of the present article as follows.

(i) The relativistic formalism of the impulse approximation has been applied to the K -REC process by incorporating the internal conversion process (ICP).

(ii) The ICP is thought to be associated with the breakup of virtual e^+e^- pairs induced by the presence of strong electric fields into real pairs. Thus this contribution becomes dominant with an electric charge of a projectile ion being larger. This effect is very pronounced on the occasion of a U^{92+} ion bombardment.

(iii) While the theoretical total cross sections by the present method reproduce experimental results fairly well

in the case of a Xe^{54+} -Be system, it is not in good agreement with the experimental datum of a U^{92+} -Be system. This discrepancy is thought due to the employment of the approximate relativistic Coulomb wave function (the Sommerfeld-Maue wave function) instead of the exact one.

(iv) Normalized photon angular distributions have been calculated up to the ultrarelativistic velocity domain ($|\mathbf{v}| \sim 1$) with consideration of a photon polarization angle ϕ . Emitted photons distribute asymmetrically as $\cos^2(\theta_L/2)$ at the very-high-velocity limit. This tendency is quite different from the conventional $\sin^2\theta_L$ dependence which holds correctly at most up to $|\mathbf{v}| \sim 0.9$. The radiation pattern at $\phi=90^\circ$ differs much from that at $\phi=0^\circ$ and at $\phi=45^\circ$.

(v) Calculations have been also made on a linear polarization correlation $P(\theta_L)$ of a photon. This quantity reflects the polarization direction of an emitted photon. The polarization direction tends to turn from on the scattering plane into the plane perpendicular to it with increasing velocity. Above $|\mathbf{v}|=0.8$, the crossover feature, the sign inversion of $P(\theta_L)$, comes out. Aside from both the forward and the backward emission angles, $P(\theta_L)$ is influenced little by the Z_p effects.

*Present address: Institute of Applied Physics, University of Tsukuba, 1-1 Tennoudai, Tsukuba-shi, Ibaraki 305, Japan.

¹E. Spindler, H.-D. Betz, and F. Bell, Phys. Rev. Lett. **42**, 832 (1979).

²R. Anholt, S. A. Andriamonje, E. Morenzoni, Ch. Stoller, J. D. Molitoris, W. E. Meyerhof, H. Bowman, J.-S. Xu, Z.-Z. Xu, J. O. Rasmussen, and D. H. H. Hoffmann, Phys. Rev. Lett. **53**, 234 (1984).

³K. Hino and T. Watanabe, Phys. Rev. A **36**, 581 (1987).

⁴K. Hino and T. Watanabe, Phys. Rev. A **36**, 5862 (1987).

⁵L. D. Landau and E. M. Lifshitz, *The Classical Theory of Fields*, Vol. 2 of *Course of Theoretical Physics*, 4th ed. (Pergamon, New York, 1975), p. 119; V. B. Berestetskii, E. M. Lifshitz, and L. P. Pitaevskii, *Quantum Electrodynamics*, Vol. 4 of *Course of Theoretical Physics*, 2nd ed. (Pergamon, New York, 1982), p. 160.

⁶For instance, G. Soff, J. Reinhard, B. Müller, and W. Greiner, Phys. Rev. Lett. **38**, 592 (1977); W. Greiner, B. Müller, and J. Rafelski, *Quantum Electrodynamics of Strong Fields* (Springer-Verlag, Berlin, 1985), p. 366.

⁷J. Macek and R. Shakeshaft, Phys. Rev. A **22**, 144 (1980); J. Macek and S. Alston, *ibid.* **26**, 250 (1982); S. Alston, *ibid.* **27**, 2342 (1983).

⁸M. Gorris, J. S. Briggs, and S. Alston, J. Phys. B **16**, L665 (1983).

⁹M. Kleber and D. H. Jakubassa, Nucl. Phys. A **252**, 152 (1975).

¹⁰D. H. Jakubassa-Amundsen, R. Hoppler, and H.-D. Betz, J. Phys. B **17**, 3943 (1984); D. H. Jakubassa-Amundsen, *ibid.* **20**, 325 (1987).

¹¹J. D. Dollard, J. Math. Phys. **5**, 292 (1960).

¹²K. Hino (unpublished); D. H. Jakubassa-Amundsen (private communication). The contents of this statement were derived by applying the Dollard technique to the near-on-shell Coulomb wave function, which has an analytical product form of the Coulomb off-shell factor and the conventional Coulomb wave function (cf. Ref. 7). However, a more rigorous proof should be made by beginning with the general integral representation of the SPB wave function (the off-shell Coulomb wave function), not the near-on-shell one, and by incorporating the asymptotic Coulomb tail with it. In this sense, the statement in the text might be temporal. Because of mathematical difficulties, this program has not been carried out so far. Since in the usual REC the off-shell energy, equal to a binding energy of an initial target electron, is very small compared with the kinetic energy of an intermediate electron, it is thought correct to approximate the exact SPB

- wave function by its analytical product form. Thus, at least, in the case of the REC, the original SPB formalism (Ref. 8) might be invalid and the IA formalism (Ref. 9) correct.
- ¹³V. B. Berestetskii, E. M. Lifshitz, and L. P. Pitaevskii, *Quantum Electrodynamics*, Vol. 4 of *Course of Theoretical Physics*, 2nd ed. (Pergamon, New York, 1982), p. 144.
- ¹⁴H. A. Bethe and E. E. Salpeter, *Quantum Mechanics of One- and Two-Electron Atoms* (Academic, New York, 1957), pp. 34 and 74.
- ¹⁵E. M. Rose, *Relativistische Elektronentheorie* (BI Hochschultaschenbücher, Mannheim, 1971).
- ¹⁶L. D. Landau and E. M. Lifshitz, *The Classical Theory of Fields*, Vol. 2 of *Course of Theoretical Physics*, 4th ed. (Pergamon, New York, 1975), p. 119; V. B. Berestetskii, E. M. Lifshitz, and L. P. Pitaevskii, *Quantum Electrodynamics*, Vol. 4 of *Course of Theoretical Physics*, 2nd ed. (Pergamon, New York, 1982), p. 24.
- ¹⁷B. C. Nagel, *Ark. Fys.* **18**, 1 (1960); R. H. Pratt, R. D. Levee, R. L. Pexton, and W. Aron, *Phys. Rev.* **134**, A898 (1964); **134**, A916 (1964).
- ¹⁸A. Nordsieck, *Phys. Rev.* **93**, 785 (1954).
- ¹⁹F. Sauter, *Ann. Phys. (Leipzig)* **9**, 217 (1931); **11**, 454 (1931); see also V. B. Berestetskii, E. M. Lifshitz, and L. P. Pitaevskii, *Quantum Electrodynamics*, Vol. 4 of *Course of Theoretical Physics*, 2nd ed. (Pergamon, New York, 1982), p. 212.
- ²⁰J. S. Briggs and K. Dettmann, *Phys. Rev. Lett.* **33**, 1123 (1974).
- ²¹S. Karashima, K. Hino, and T. Watanabe, *J. Phys. Soc. Jpn.* (to be published).
- ²²In Ref. 3, we considered these differences were due to Coulomb off-shell factors originating from the SPB theory. In accordance with statements of Refs. 10 and 12, however, this conclusion is incorrect.
- ²³Setting $|\mathbf{v}|$ equal to 1, and v_p and v_r to 0 in the present RIA formalism, we can obtain this analytic form of a photon angular distribution at the ultrarelativistic high-energy limit. But the Sauter formula of Ref. 19 cannot be applied to such a high incident energy region because this provides meaningless negative cross sections as well as does not give the proper $\cos^2(\theta_L/2)$ dependence.